Journal of Cerebral Blood Flow & Metabolism (2013) 33, 322–329

www.jcbfm.com

FEATURE ARTICLE

# *In vivo* detection of cerebral cortical microinfarcts with high-resolution 7T MRI

Susanne J van Veluw[1], Jaco JM Zwanenburg[2], JooYeon Engelen-Lee[3], Wim GM Spliet[3], Jeroen Hendrikse[2], Peter R Luijten[2] and Geert Jan Biessels[1]

Cerebrovascular disease has an important role in cognitive decline and dementia. In this context, cerebral microinfarcts are attracting increasing attention, but these lesions could thus far not be detected *in vivo*. The aim of this study was to try to identify possible cortical microinfarcts on high-resolution 7T *in vivo* magnetic resonance imaging (MRI) and to perform a histopathologic validation study on similar appearing lesions on 7T *ex vivo* MRI of postmortem brain tissue. The study population consisted of 22 elderly subjects, who underwent 7T MRI. The fluid attenuated inversion recovery, $T_2$, and $T_1$ weighted scans of these subjects were examined for possible cortical microinfarcts. In the *ex vivo* MRI study, 15 formalin-fixed coronal brain slices of 6 subjects with Alzheimer and vascular pathology were examined and subjected to histopathologic verification. On the *in vivo* scans, 15 cortical lesions could be identified that were likely to be microinfarcts in 6 subjects. In the postmortem tissue, 6 similar appearing lesions were identified of which 5 were verified as cortical microinfarcts on histopathology. This study provides strong evidence that cortical microinfarcts can be detected *in vivo*, which will be of great value in further studies into the role of vascular disease in cognitive decline and dementia.

*Journal of Cerebral Blood Flow & Metabolism* (2013) **33,** 322–329; doi:10.1038/jcbfm.2012.196; published online 19 December 2012

**Keywords:** brain; histology; magnetic resonance imaging; microinfarcts; small vessel disease

## INTRODUCTION

Cognitive decline and dementia are major manifestations of cerebrovascular disease. Approximately one in five patients with acute stroke develops dementia within a year after stroke.[1] Even more often, cerebrovascular disease is involved in cognitive decline or dementia in people without an obvious history of stroke. Autopsy studies identify vascular pathology in the majority of patients with dementia, also in those with a clinical diagnosis of Alzheimer's disease (AD).[2,3] This vascular pathology frequently involves the small vessels of the brain, including small arteries and arterioles, but also capillaries and small veins, and is referred to as cerebral small vessel disease (SVD).[4] Imaging correlates of SVD on conventional brain magnetic resonance imaging (MRI) include lacunar infarctions, white matter hyperintensities (WMHs), and microbleeds.[4] Importantly, these MRI lesions do not fully capture the burden of vascular damage in aging and dementia. In this context, cerebral microinfarcts (CMIs) are attracting increasing attention. They are considered to be the single most widespread form of brain infarction and thus a major component of the causal pathway between SVD and cognitive dysfunction.[5,6] On autopsy, CMIs are observed in around 43% in patients with AD, 62% in patients with vascular dementia, and 24% in nondemented elderly subjects.[6] Cerebral microinfarcts are typically defined as sharply delineated microscopic ischemic lesions accompanied by cellular death or tissue necrosis, often associated with gliosis and cavitation.[2,7] Cerebral microinfarcts can occur in both the white-matter and (sub)cortical regions of the brain, presumably more so in watershed areas.[6,8] Because of their small sizes (ranging from 50 $\mu$m to a few mm), CMIs escape detection by regular clinical MRI protocols. With the introduction of high field strength (7.0 T) MRI, which allows high-resolution imaging with isotropic voxel sizes in the submillimeter range, CMIs may be visualized *in vivo*. The aim of this study was to try to identify possible CMIs on 7.0 T magnetic resonance (MR) images of elderly subjects without a known history of dementia, and to perform a histopathologic validation study on similar appearing lesions on 7.0 T MR images of postmortem brain tissue that met the same criteria as *in vivo*.

## MATERIALS AND METHODS

### Study Population

Functionally independent elderly subjects, aged between 65 and 80, were recruited through their general practitioners. Exclusion criteria were contraindications for 7.0 T MRI (e.g., claustrophobia, metal objects such as dental implants or prostheses in or on the body), or a known psychiatric or neurologic disorder that could influence cognitive functioning, including recent nondisabling stroke (<2 years) or any disabling stroke, major depression or a history of alcohol or substance abuse. Subjects underwent a Mini-Mental State Examination[9] and had to have a score of 26 or higher for inclusion in the present study. General practitioners made a first selection against these criteria. In the period of October 2010 to 2011, 54 eligible subjects were willing to participate in the study. Twenty-two were excluded because of MR contraindications, and another eight because of other reasons. Hence, 24 individuals were included in this study. They all underwent 7.0 T MRI scanning in the University Medical

[1]Department of Neurology, Rudolf Magnus Institute of Neuroscience, University Medical Center Utrecht, Utrecht, The Netherlands; [2]Department of Radiology, University Medical Center Utrecht, Utrecht, The Netherlands and [3]Department of Neuropathology, University Medical Center Utrecht, Utrecht, The Netherlands. Correspondence: SJ van Veluw, Department of Neurology, University Medical Center Utrecht G03.232, P.O. Box 85500, GA 3508 Utrecht, The Netherlands.
E-mail: s.j.veluw-2@umcutrecht.nl
This work was supported by a VIDI grant from ZonMw, The Netherlands Organisation for Health Research and Development (grant number 91711384), and a grant from the Netherlands Heart Foundation (grant number 2010T073) to GJB.
Received 3 September 2012; revised 31 October 2012; accepted 31 October 2012; published online 19 December 2012

Center Utrecht (UMCU, The Netherlands) with the same standardized protocol including fluid attenuated inversion recovery (FLAIR), a $T_2$ weighted, and a $T_1$ weighted sequence. The scans of two subjects could not be used because of severe motion artifacts. This resulted in a study population of 22 subjects.

The study was approved by the medical ethics committee of the UMCU and all subjects gave written informed consent according to the Declaration of Helsinki.

### *In Vivo* Magnetic Resonance Imaging Scanning Protocol

Scans were acquired on a whole-body 7.0 T MR system (Philips Healthcare, Cleveland, OH, USA) with a volume transmit and 16-channel receive head coil (Nova Medical, Wilmington, MA, USA). Subjects included in the study later than May 2011 (nine in total) were scanned with a volume transmit and 32-channel receive head coil (Nova Medical), which, as far as we could judge, did not cause any observable differences in lesion appearance. The standardized protocol included the following sequences:

(i) Volumetric (3D) magnetization prepared FLAIR with an acquired, isotropic resolution of $0.8 \times 0.8 \times 0.8\,mm^3$, repetition time (TR) = 8,000 ms, nominal echo time (TE) = 300 ms using constant low refocusing angles of 70°, inversion time (TI) = 2,325 ms, matrix size = $312 \times 304$.[10] Scan duration was 12 minutes 48 seconds.
(ii) 3D $T_2$ weighted turbo-spin echo with an acquired, isotropic resolution of $0.7 \times 0.7 \times 0.7\,mm^3$, TR = 3,158 ms, nominal TE = 301 ms with a variable refocusing flip angle sweep,[11,12] leading to an equivalent TE (for $T_2$ contrast) of ~57 ms for gray and white matter, matrix size = $356 \times 357$. Scan duration was 10 minutes 15 seconds.
(iii) 3D $T_1$ weighted sequence with an isotropic resolution of $1.0 \times 1.0 \times 1.0\,mm^3$, flip angle 8°, TR = 4.8 ms, TE = 2.2 ms, TI = 1,240 ms, TR of the inversion pulses = 3,500 ms, matrix size = $200 \times 250$. Scan duration was 1 minute 57 seconds.

All subjects also underwent a 3.0 T MRI (Intera, Philips, Best, The Netherlands) on the same day, which included the following sequences:

(i) 2D multislice FLAIR with 48 slices, with an acquired resolution of $1.0 \times 1.3 \times 3.0\,mm^3$, TR = 11,000 ms, TE = 125 ms, TI = 2,800 ms, matrix size = $232 \times 148$. Scan duration was 2 minutes 56 seconds.
(ii) 2D $T_2$ weighted dual echo turbo-spin echo with 48 slices, with an acquired resolution of $1.0 \times 1.1 \times 3.0\,mm^3$, TR = 3,198 ms, TE1 = 19 ms, TE2 = 140 ms, matrix size = $232 \times 179$. Scan duration was 2 minutes 43 seconds.
(iii) 3D $T_1$ weighted turbo-field echo with 192 slices, with an acquired resolution of $1.0 \times 1.0 \times 1.0\,mm^3$, flip angle 8°, TR = 7.9, TE = 4.5, TI = 955 ms, TR of the inversion pulses = 3,000 ms, matrix size = $256 \times 232$. Scan duration was 6 minutes 43 seconds.

### Magnetic Resonance Imaging Rating

Histopathologically, CMIs have been described as sharply delineated microscopic ischemic lesions, often associated with gliosis and cavitation.[2,7] Based on those features, we hypothesized that on ultra-high resolution MRI CMIs would appear as small hyperintense circumscript—with or without a hypointense center—lesions on FLAIR, hyperintense on $T_2$ weighted, and hypointense or isointense on $T_1$ weighted images. We focused on CMIs in the cerebral cortex, because autopsy studies indicate that these lesions are particularly common in the cortex. Moreover, we expected that in the subcortical gray and white matter it would be more difficult to differentiate CMIs from other focal lesions including perivascular spaces and punctate WMHs (i.e., small focal hyperintensities on $T_2$[13]).

In an initial evaluation the FLAIR scans (sagittal view) of all subjects were thoroughly examined to identify possible cortical CMIs and the findings were compared with $T_2$ weighted and $T_1$ weighted scans. During this process, we did identify multiple hyperintense cortical lesions suspected to be CMIs on FLAIR, but we did not see lesions with a hypointense center. In all cases, these hyperintense FLAIR lesions were hyperintense on $T_2$ weighted and hypointense on the corresponding $T_1$ weighted scan. Based on this initial evaluation, we operationally defined possible cortical CMIs on 7.0 T MRI for further visual rating as hyperintense on FLAIR, hyperintense on $T_2$ weighted, and hypointense on $T_1$ weighted scans. Each lesion had to be detectable on all three views of the brain (sagittal, coronal, and transversal), and restricted to the cortex. Moreover, they had to be distinct from perivascular spaces. We observed that some perivascular spaces extended from the white matter into the cortex, producing changes in cortical signal intensities mimicking those of possible CMIs. Therefore, we discarded all small cortical lesions that were in direct contact with a perivascular space in the underlying white matter as possible CMIs. Based on those criteria, the MR images of all subjects were reevaluated systematically and possible cortical CMIs were scored. All identified possible cortical CMIs were inspected by a second rater, experienced in the field of neuroradiology. Both raters were blinded to clinical information such as age. In the case of disagreement, for every location consensus was reached.

When a possible cortical CMI was identified on 7.0 T, the corresponding 3.0 T FLAIR, $T_2$, and $T_1$ weighted images were examined at the same location. This was performed by visual inspection using landmarks.

In addition, WMHs were assessed on the 3.0 T FLAIR images using the Age Related White Matter Changes scale,[13] by two independent raters. Lacunar infarctions were also identified.

### Postmortem Tissue

For *ex vivo* MRI protocol optimization three formalin-fixed 10-mm thick coronal brain slices were used. These slices, provided by the anatomy department of the UMCU, were from subjects who had donated their brains to science; therefore, detailed subject information was unavailable.

**Table 1.** Subject and tissue characteristics of the *ex vivo* study

| *Subject* | *Neuropathologic diagnosis*[a] | *Sex F/M* | *Age (years)* | *Number of slices* | *Fixation duration (months)* | *Number of CMIs*[b] *Ex vivo MRI* | *Number of CMIs*[c] *Histology* |
|---|---|---|---|---|---|---|---|
| A | AD (B&B VI) | F | 64 | 4 | 6 | 1 | 1 |
| B | Lewy body dementia (B VI) | M | 83 | 3 | 3 | 1 | 0 |
| C | AD (B&B VI) with hypertensive vasculopathy (with hemorrhagic infarct) | M | 74 | 2 | 9 | 1 | 1 |
| D | Extensive hypoxic-ischemic brain damage (with early stage of infarction in the watershed areas) | M | 71 | 2 | 15 | 1 | 1 |
| E | Alpha-synucleinopathy, classified as Lewy body dementia (B III-IV) | M | 87 | 2 | 14 | 0 | 0 |
| F | AD (B&B II) with mild-to-severe hypoxic-ischemic brain damage (with cystic degeneration of infarct in the left operculum as a result of atherosclerotic vasculopathy) | M | 79 | 2 | 6 | 4[d] | 6[e] |

CMI, cerebral microinfarct; F, female; M, male; AD, Alzheimer's disease; B&B, Braak & Braak stage;[29] B, Braak stage;[30] MRI, magnetic resonance imaging. [a]Neuropathologic diagnosis was established on whole-brain and targeted histopathologic examination. [b]Number of possible CMIs identified on *ex vivo* MRI. [c]Number of definite CMIs verified on histopathologic examination. [d]Two cortical CMIs in the brain tissue of this subject were solely found on ultra-high resolution *ex vivo* $T_2$ ($400 \times 400 \times 400\,\mu m^3$) in retrospect, after the CMI was identified on histopathologic examination. [e]One cortical CMI was found in the negative control tissue taken from the brain tissue of this subject (and could not be found again on *ex vivo* MRI). One additional CMI was found in close proximity to one of the CMIs that was identified on *ex vivo* MRI. These extra CMIs could in retrospect not be found on *ex vivo* MRI.

Initially, we scanned with the tissue submerged in Fomblin (Solvay Solexis, Bollate, Italy), a proton-free fluid without MR signal. Later, we scanned the tissue submerged in 4% formaldehyde solution (formalin). After careful comparison of MR image quality, it was decided to use formalin during scanning, which proved to provide better tissue-fluid contrast.

After protocol optimization, 15 formalin-fixed 10-mm thick coronal brain slices from six subjects were submitted to *ex vivo* MRI. These subjects had undergone autopsy in our hospital, after informed consent of the family was obtained. Patients were selected from the database of the neuropathology department based on reported cerebrovascular and Alzheimer pathology on autopsy. Details of subject and brain tissue characteristics are provided in (Table 1).

At least 2 hours in advance of scanning two coronal brain slices were placed in a plastic container, submerged in formalin. Care was taken to avoid air bubbles. Before scanning, the plastic container was sealed in a plastic bag, wrapped in a towel, and placed in the center of the MR head coil. The use of the material of these patients for this study was in accordance with local regulations and approved by the medical ethics committee of the UMCU.

### *Ex Vivo* Magnetic Resonance Imaging Scanning Protocol

Scans were acquired overnight on the same whole-body 7.0 T MR system as the *in vivo* scans, with a volume transmit and 32-channel receive head coil (Nova Medical). We used two different protocols. The first *ex vivo* protocol included the same sequences as *in vivo* (FLAIR and $T_2$ weighted, with exception of the $T_1$ weighted) and is referred to as 'clinical resolution protocol.' The TI was adjusted to obtain proper nulling of the formalin, in which the postmortem tissue was submerged during scanning. Also the refocusing angle was reduced, to account for the fact that the relaxation times of formalin-fixed tissue are more reduced as compared with *in vivo* tissue.

The second protocol aimed to obtain an even higher resolution and is referred to as 'ultra-high resolution protocol.' In this ultra-high resolution protocol, the postmortem tissue was scanned with the following parameters:

(i) 3D FLAIR with an acquired isotropic resolution of $400 \times 400 \times 400$ $\mu m^3$, TR = 8,000 ms, nominal TE = 164 ms using constant low refocusing angles of 40°, TI = 1,600 ms, matrix size = $500 \times 280$. Scan duration was 4 hours 16 minutes 8 seconds.
(ii) $T_2$ weighted turbo-spin echo with an acquired isotropic resolution of $400 \times 400 \times 400$ $\mu m^3$, TR = 3,500 ms, nominal TE = 164 ms using constant low refocusing angles of 40°, matrix size = $500 \times 280$. Scan duration was 1 hour 52 minutes 3 seconds.
(iii) $T_2$* weighted sequence with an isotropic acquired resolution of $180 \times 180 \times 180$ $\mu m^3$, flip angle 25°, TR = 75 ms, TE = 20 ms, matrix size = $832 \times 834$. Scan duration was 4 hours 59 minutes 31 seconds.

### Sampling Procedure and Histology

The sampling procedure was established in three formalin-fixed 10-mm thick coronal brain slices, derived from subjects who had donated their brains to science (Figure 1). After this development stage, the following procedure was performed on the brain tissue of the patients used in this study: after the *ex vivo* MRI scanning session, blocks of tissue ($20 \times 10 \times 0.5$ $mm^3$) were cut from the sites where possible cortical CMIs were detected on the *ex vivo* MR images. All lesions that presented as cortical hyperintensities on both the clinical and ultra-high resolution *ex vivo* FLAIR as well as the $T_2$ weighted images were sampled. The ultra-high resolution $T_2$* weighted sequence provided an extra level of detail and therefore served as a useful guide for sampling. As a negative control, two blocks of tissue in two different brain slices of two different subjects were cut from a site where no lesion was visible on any MR image. All blocks were dehydrated and preprocessed, after which they were embedded in paraffin. Further, 4-$\mu$m thick serial sections were cut using a microtome. Standard histologic staining was performed on these sections, which included a hematoxylin/eosin (for cell bodies) stain, and a Luxol fast blue & Periodic acid-Schiff (for myelin) stain. Sections were studied under a Carl Zeiss microscope, and photographs were obtained with a digital camera, mounted on top of the microscope. Sections were examined by the neuropathologist of our hospital. Cortical CMIs were determined based on the presence of a sharply delineated area of ischemia, cellular death, and tissue necrosis. Furthermore, the presence of gliosis and cavitation was noted, and lesion diameter was measured on the obtained photograph.

## RESULTS

### *In Vivo* 7.0 T Magnetic Resonance Imaging

The 22 subjects included in this study had a mean age of $68.7 \pm 3.2$ years and a median Mini-Mental State Examination score of 29 (range 26 to 30). A total number of 15 lesions that met

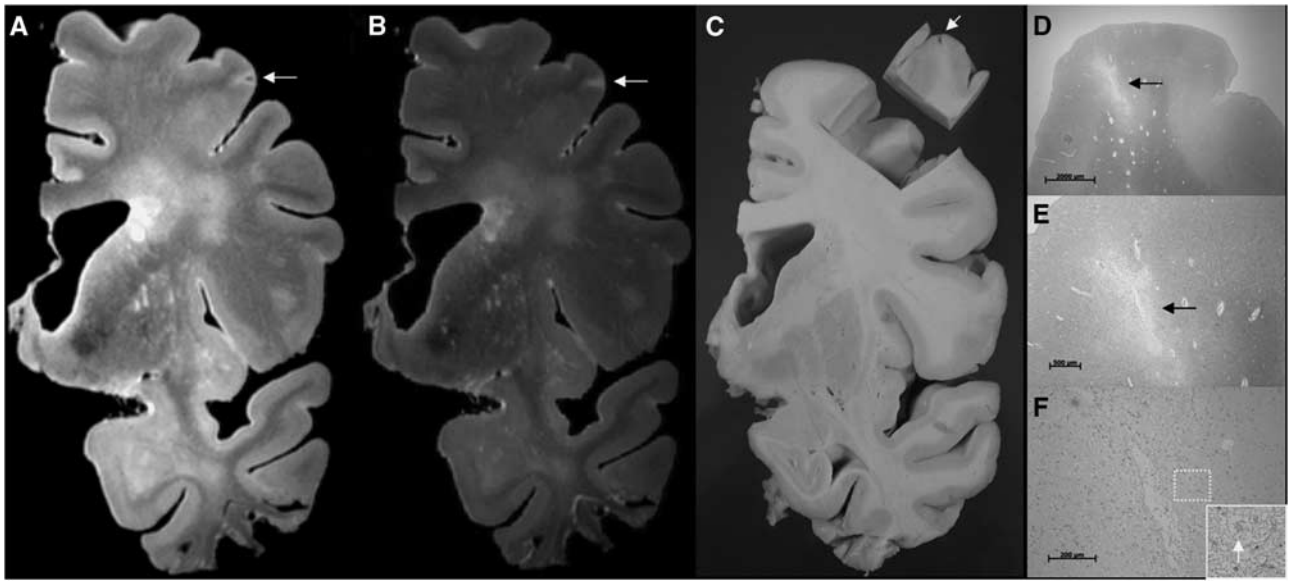


**Figure 1.** Sampling procedure: correlation of *ex vivo* magnetic resonance imaging (MRI) and histology. The sampling procedure was developed in three brain slices from anonymous donors. In one of these brain slices a cortical lesion of interest, presumed to be ischemic, was identified on *ex vivo* MRI. This lesion appeared as a hyperintense cortical lesion with a hypointense center on a fluid attenuated inversion recovery (FLAIR) (**A**; $400 \times 400 \times 400$ $\mu m^3$), and as a hyperintense cortical lesion on a $T_2$ weighted (**B**; $400 \times 400 \times 400$ $\mu m^3$) magnetic resonance (MR) image. After dissection of the tissue for sampling a cavity in the cortex was visible (**C**; tissue block is turned over). On histopathologic examination, this cortical lesion was identified as a cerebral microinfarct (CMI) with cavitation and gliosis in the surrounding tissue (**D**, and in greater detail **E**) (Luxol fast blue & Periodic acid-Schiff (L&P) stain). On higher magnification, gliosis is visible (**F**; arrow indicates a reactive astrocyte) (hematoxylin/eosin (HE) stain). Tissue was submerged in Fomblin.

our criteria for possible cortical CMIs were identified (see for examples, Figures 2 and 3) in 6 of 22 subjects (27.3%). Four subjects had one possible cortical CMI, one subject had two possible cortical CMIs, and one subject had nine possible cortical CMIs. There were no clear differences in subject characteristics, WMH load and presence of lacunar infarctions between subjects with or without CMIs (Table 2).

Possible cortical CMIs appeared as sharply delineated linear lesions, perpendicular to the cortical surface and extending into the lower cortical layers. All identified possible cortical CMIs were $\leqslant 3$ mm. They were primarily identified in the parietal and frontal cortical regions (one possible cortical CMI was located in the occipital cortex). One subject had several small hyperintense cortical lesions on FLAIR and $T_2$ presumed to be of ischemic origin in the occipital cortex, but these were not classified as possible CMIs, because they were related to a larger area of infarction. The temporal lobes proved difficult to assess, because of a low signal-to-noise ratio in these areas, which is a current known limitation of the applied 7.0 T FLAIR MR sequence.[10] Of all possible cortical CMIs, the corresponding location on 3.0 T FLAIR, $T_2$, and $T_1$ was examined. Of the 15 possible cortical CMIs identified at 7.0 T, one was visible on both the corresponding 3.0 T $T_2$ and $T_1$ (Supplementary Figure), another three were solely visible on the corresponding 3.0 T $T_1$, but none were visible at the corresponding 3.0 T FLAIR.

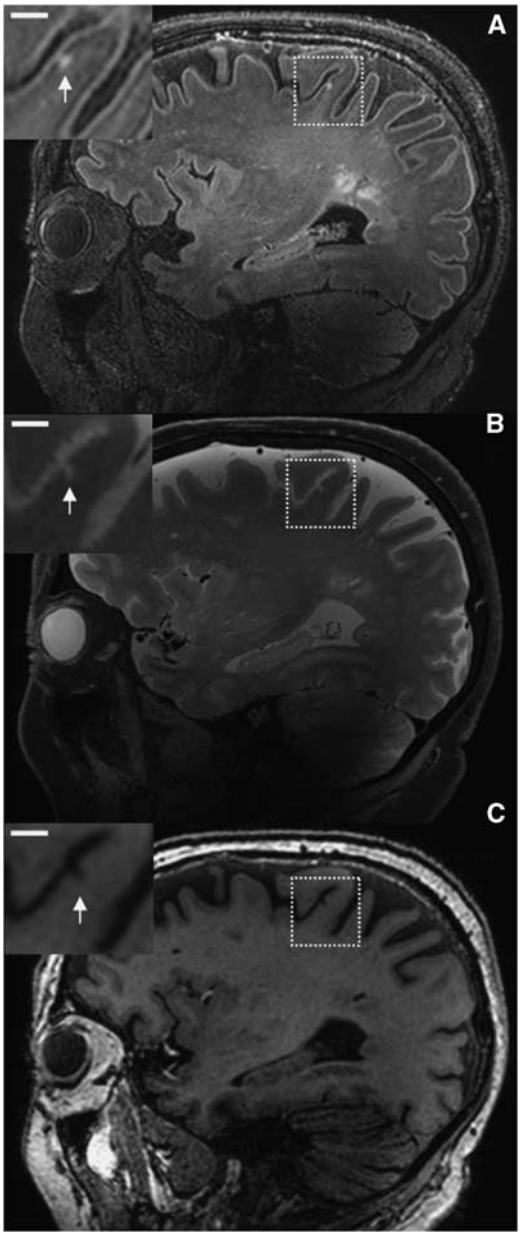


**Figure 2.** Possible cerebral microinfarct (CMI) at 7.0 T *in vivo* magnetic resonance imaging (MRI). A possible cortical CMI in a 76-year-old nondemented male is represented as a hyperintense cortical lesion on a fluid attenuated inversion recovery (FLAIR) (**A**; $0.8 \times 0.8 \times 0.8\,mm^3$) and a $T_2$ weighted (**B**; $0.7 \times 0.7 \times 0.7\,mm^3$), and as a hypointense lesion on a $T_1$ weighted (**C**; $1.0 \times 1.0 \times 1.0\,mm^3$) magnetic resonance (MR) image on a sagittal view of the brain. Scale bar indicates 4 mm.

*Ex Vivo* 7.0 T Magnetic Resonance Imaging

Characteristics and autopsy findings of the six subjects whose brain slices were used for *ex vivo* MRI are provided in Table 1. In 15 slices, a total of six hyperintense cortical lesions were identified on the ultra-high as well as on the clinical resolution FLAIR and $T_2$ *ex vivo* MR images. Appearance of the lesions was similar to the possible CMIs on *in vivo* MRI. The six lesions were sampled and further processed. At histopathologic examination, all but one of these lesions could be identified on the corresponding section. On microscopy all five lesions that were identified appeared as focal lesions of pallor with cellular death, attributed to ischemia, and moderate gliosis in the surrounding tissue (Figure 4). Based on these distinctive characteristics, these ischemic lesions were classified by the neuropathologist as definite CMIs. Their sizes varied from $\sim$1,200 to 2,500 $\mu$m as measured on the obtained microscopic photographs.

Microscopic examination identified three additional small cortical CMIs that were not identified on the initial visual inspection of the *ex vivo* MRI. Two of these CMIs could be identified after reinspection of the *ex vivo* MR images, on the corresponding ultra-high resolution $T_2$ weighted MR image (one is depicted in Figure 5). These CMIs measured 470 and 1,300 $\mu$m, respectively. The third CMI (780 $\mu$m) was located close to a sulcus which limited its detection, on *ex vivo* MRI, possibly because of partial volume effects. In the two blocks of tissue that were sampled from regions where no lesion was visible on the MR images (negative controls), one small cavitated cortical CMI (670 $\mu$m) was found on histopathologic examination. This cortical CMI could not be found on *ex vivo* MRI, after reinspection of the corresponding images, possible also because of a partial volume effect.

## DISCUSSION

This study shows that CMIs can be detected noninvasively during life. We observed small cortical lesions on 7.0 T MR images of nondemented elderly subjects that were compatible with our predefined features of cortical CMIs. Histopathologic validation of lesions with similar characteristics on *ex vivo* MRI showed that these lesions were indeed CMIs.

In the *ex vivo* part of this study, CMIs that appeared as focal lesions of pallor with neuronal loss, attributed to ischemia, on histology, gave a hyperintense signal on FLAIR and $T_2$ weighted *ex vivo* MR images.[2,7] In the neuropathologic literature, there is no consensus on the definition of the size of a CMI. Some studies report an upper limit for CMI size as 'microscopic' or 'not visible to the naked eye,' but several studies also classify lesions up to a few mm in size as CMIs.[5,6] Our findings suggest that with ultra-high resolution *ex vivo* 7.0 T MRI CMIs larger than 0.5 mm can be detected. With clinical resolution 7.0 T MRI (both *ex vivo* and *in vivo*) only the larger CMIs ($\geq$1 mm) can be detected. Compared with neuropathology, *in vivo* MRI has the obvious advantage that it allows (repeated) assessment of living subjects, thus allowing

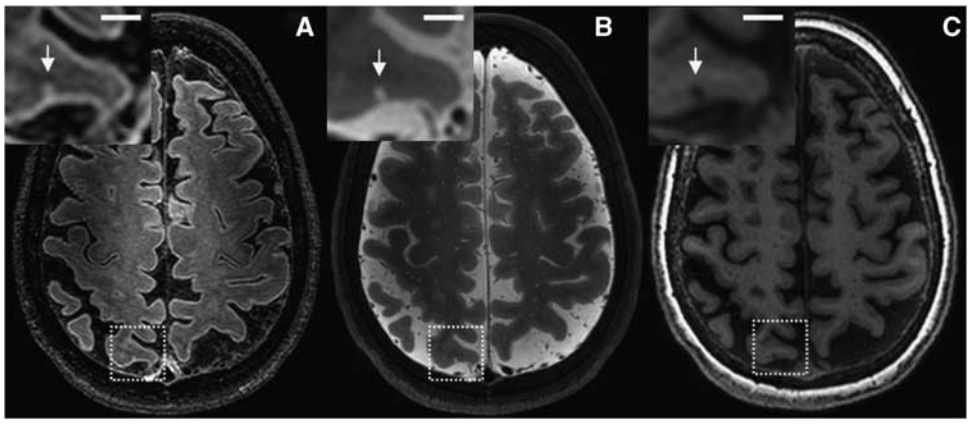


**Figure 3.** Possible cerebral microinfarct (CMI) at 7.0 T *in vivo* magnetic resonance imaging (MRI). A possible cortical CMI in a 66-year-old nondemented female is represented as a hyperintense cortical lesion on a fluid attenuated inversion recovery (FLAIR) (**A**; $0.8 \times 0.8 \times 0.8\,mm^3$) and a $T_2$ weighted (**B**; $0.7 \times 0.7 \times 0.7\,mm^3$), and as a hypointense lesion on a $T_1$ weighted (**C**; $1.0 \times 1.0 \times 1.0\,mm^3$) magnetic resonance (MR) image on a transversal view of the brain. Scale bar indicates 4 mm.

**Table 2.** Subject characteristics of the *in vivo* study

| | *With CMIs,* n = *6* | *No CMIs,* n = *16* |
|---|---|---|
| Age (years) | 70.5 ± 4.3 | 68.2 ± 2.4 |
| Male sex | 2 (33) | 7 (44) |
| Hypertension[a] | 4 (67) | 8 (50) |
| Diabetes mellitus[a] | 1 (17) | 4 (25) |
| Systolic blood pressure (mm Hg) | 136 ± 14 | 145 ± 14 |
| Diastolic blood pressure (mm Hg) | 82 ± 5 | 80 ± 5 |
| MMSE score | 29 (27–30) | 29 (26–30) |
| White matter hyperintensities | 3.5 (1–8.5) | 2.5 (0.5–17) |
| Lacunar infarctions | 3 (50) | 5 (31) |

CMI, cerebral microinfarct; MMSE, Mini-Mental State Examination.
Data are presented as mean ± SD, *n* (%), or median (range).
[a]Subjects were considered having arterial hypertension, or diabetes mellitus, if they had a known history of the disease or were receiving drug treatment for these conditions.

longitudinal studies of CMIs in relation to other clinical parameters. Another advantage is that MRI provides coverage of almost the complete brain, while histologic studies typically have to rely on sampling of only a small proportion of the brain in different areas. At the 50 $\mu$m to 0.5 mm range, however, our current MRI protocol will miss CMIs. In that perspective, the lesions that were identified with *in vivo* MRI in the current study are more likely to be the 'top of the iceberg' of total CMI load. It is yet unclear if the etiology of these smallest CMIs is identical to that of the somewhat larger lesions. Nonetheless, the prevalence of cortical CMIs in 6 of 22 (27.3%) elderly subjects in the *in vivo* part of the current study is in the same range (i.e., 24%), as the neuropathologic findings reported in nondemented elderly subjects.[6]

*Ex vivo* MRI proves to be a valuable tool in determining MR markers in brain diseases with multiple small focal abnormalities such as vascular lesions and demyelination, providing whole-brain coverage and targeted sampling for histopathologic examination.[14–16] A recent study suggested that prolonged storage (>6 years) of formalin-fixed tissue results in subtle histology artifacts, which sometimes on *ex vivo* MRI is indistinguishable from genuine brain pathology.[17] In our case, we have solely used postmortem brain tissue that has been stored for no longer than 15 months, therefore we assume our samples are not susceptible for mentioned alterations in the tissue and on the corresponding MR images.

Previously, CMIs have been identified on *ex vivo* (7.0 T) MRI in brain tissue of a single patient with CADASIL (cerebral autosomal-dominant arteriopathy with subcortical infarcts and leukoencephalopathy).[18] The brain tissue of this patient presented with several CMIs on high-resolution $T_2$* weighted scans, which were histopathologically validated.[18] Possible CMIs have recently been described in an *in vivo* MRI study at 3.0 T.[19] That study, which did not verify the nature of the observed lesions histologically, included 70 subjects with AD or cerebrovascular disease and observed small intracortical high signal lesions suspected to be CMIs on both advanced double inversion recovery and 3D FLAIR images with high in-plane resolutions in only nine subjects.[19] The lesions depicted in that paper are of similar appearance as the lesions depicted in our study, albeit of larger size. Apparently, it is also possible to detect CMIs at field strengths lower than 7.0 T, as our findings at 3.0 T also show. Probably, lesion detection at lower field strengths can be improved by further protocol optimization. We recommend that such protocols include at least heavily $T_2$ weighted FLAIR, $T_2$, and $T_1$ weighted sequences. A separate study would be needed to investigate to what extent our 7.0 T results can be translated to 3.0 T MRI, and how a 3.0 T protocol should be optimized for this purpose. However, we expect that 7.0 T definitely is more sensitive for CMI detection compared with 3.0 T, either by an increased signal-to-noise ratio, improved contrast, a higher resolution, or by a combination of these factors.[20]

Cerebral microinfarcts have been studied extensively in neuropathologic studies. A systematic review of 32 of these studies, involving neuropathologic data of over 10,000 subjects, emphasized the potential clinical relevance of CMIs.[6] Cerebral microinfarcts are an important correlate of aging-related cognitive impairment and dementia and vascular disease.[7,21–24] Although they are small, autopsy data suggest that CMIs might be the most widespread form of brain infarction and are thus conceivable to cause substantial clinical symptoms.[5,25,26] In a clinicopathologic study examining the brains of 285 autopsied decedents as part of the HAAS (Honolulu-Asia Aging Study), it was found that neither large infarcts, lacunar infarctions, nor hemorrhages added significantly to the variance in the final antemortem cognitive test score as established by the CASI (Cognitive Abilities Screening Instrument). Only CMIs were independently associated with poor CASI test scores.[7] While the role of CMIs in aging and dementia is increasingly recognized, the underlying pathophysiology of CMIs

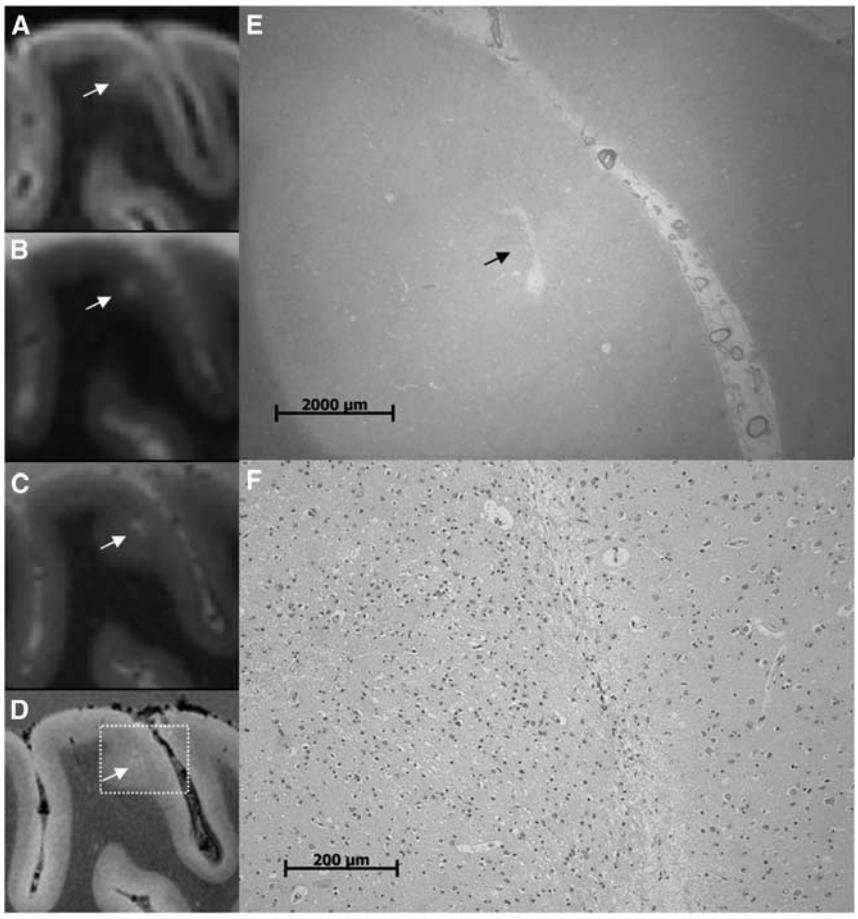


**Figure 4.** A cerebral microinfarct (CMI) identified with *ex vivo* magnetic resonance imaging (MRI). A CMI in a formalin-fixed coronal brain slice of a 64-year-old patient with a neuropathologic diagnosis of Alzheimer's disease (AD). The CMI is presented as a hyperintense cortical lesion on a clinical resolution fluid attenuated inversion recovery (FLAIR) (**A**; $0.8 \times 0.8 \times 0.8\,mm^3$) and a clinical resolution $T_2$ weighted image (**B**; $0.7 \times 0.7 \times 0.7\,mm^3$), and as a hyperintense cortical lesion in greater detail on an ultra-high resolution $T_2$ weighted (**C**; $400 \times 400 \times 400\,\mu m^3$) magnetic resonance (MR) image. On an ultra-high resolution $T_2$* weighted (**D**; $180 \times 180 \times 180\,\mu m^3$) MR image, the CMI can be observed in even greater detail and in close resemblance to the microscopic images in (**E**) and (**F**). On histopathologic examination, this cortical lesion was established as a CMI with moderate gliosis in the surrounding tissue (**E**; Luxol fast blue & Periodic acid-Schiff (L&P) stain, and in greater detail **F**; hematoxylin/eosin (HE) stain).

is not completely understood. A recent neuropathologic study suggests that CMIs are an end stage of microvascular pathology in SVD.[27] Now CMIs prove to be detectable noninvasively during life, as shown in the present study, the clinical significance, etiology, and prognostic value of CMIs can be further established. Our study was designed to assess the possibility to detect CMIs *in vivo*, and cannot yet address these issues. Our findings thus set the stage for further studies on CMIs in larger samples of patients with different clinical diagnoses and on the relation between CMIs and cognitive functioning and other SVD correlates, such as lacunar infarctions, WMHs, and microbleeds.

The strength of this work is the use of advanced imaging technique in a combined *in vivo–ex vivo* correlation study. Our study does also have several limitations. First of all, the histopathologic verification of the possible CMIs detected *in vivo* relied on autopsy material of other subjects. Moreover, while the *in vivo* study concerned nondemented healthy elderly subjects, postmortem tissue of patients with Alzheimer and vascular pathology was used for the *ex vivo* validation study. We specifically decided to focus on patients with advanced pathology in the *ex vivo* study because we wanted to enrich our sample for microvascular pathology, thus increasing the chances of finding lesions in a limited number of brain slices. Nevertheless, based on the current literature there is no evidence that the key histologic features of CMIs differ between people with or without dementia. Furthermore, the operational definition of CMIs is derived from the set of subjects in this study and applied to the same set. This definition might have to be adjusted in the future, or extended for other subtypes of CMIs, based on emerging insights from further studies on *in vivo* and *ex vivo* MRI. Another limitation was that the *ex vivo* scanning protocol did not include a $T_1$ weighted sequence. As $T_1$ relaxation in formalin-fixed tissue is severely reduced compared with *in vivo* it proved difficult to develop such a sequence resembling the *in vivo* state.[28] Finally, there are still strict safety regulations for 7.0 T MRI that may have led to selection bias in the *in vivo* study.

## Conclusion

By combining high-resolution *in vivo* MRI and *ex vivo* MRI with histologic verification, this study provides strong evidence that cortical CMIs can be detected *in vivo*. Cortical CMIs are thus a novel *in vivo* marker of SVD that can be of great value in further studies into the role of vascular disease in aging-related cognitive decline and dementia.

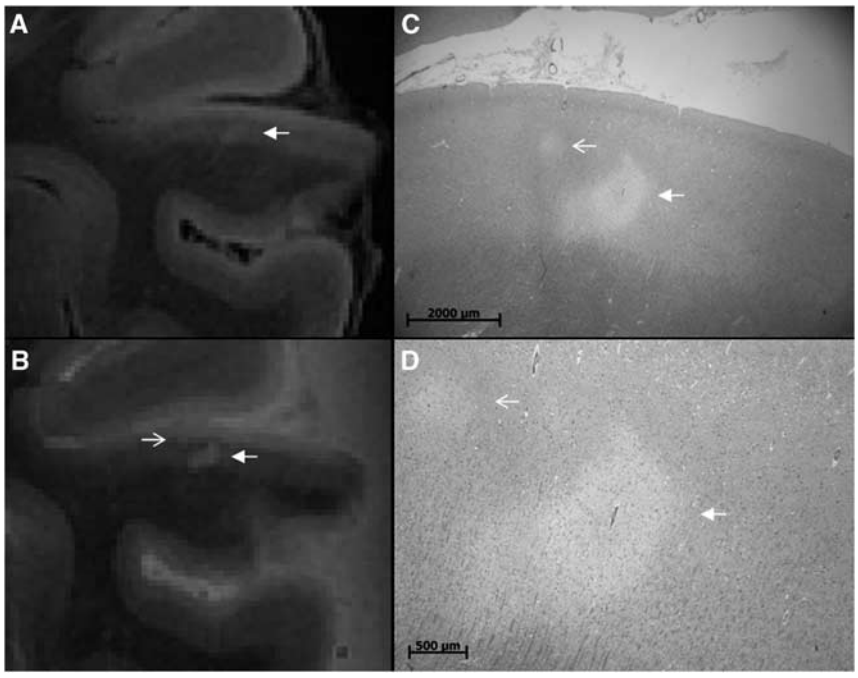


**Figure 5.** An additional cerebral microinfarct (CMI) identified with histology. A CMI in a formalin-fixed coronal brain slice of a 79-year-old patient with Alzheimer's disease (AD) pathology. The CMI is presented as a hyperintense cortical lesion on an ultra-high resolution fluid attenuated inversion recovery (FLAIR) (**A**; arrow; $400 \times 400 \times 400\ \mu m^3$) and an ultra-high resolution $T_2$ weighted (**B**; arrow; $400 \times 400 \times 400\ \mu m^3$) magnetic resonance (MR) image. On histopathologic examination, this cortical lesion was established as a CMI (**C**, Luxol fast blue & Periodic acid-Schiff (L&P) stain, and in greater detail **D**, L&P stain). Note the smaller CMI in (**C**) and (**D**) (open arrow) which was initially solely identified on histopathologic examination, but at reinspection proved to be visible on the ultra-high resolution $T_2$ weighted MR image as well (**B**; open arrow).

## DISCLOSURE/CONFLICT OF INTEREST

The authors declare no conflict of interest.

## ACKNOWLEDGEMENTS

The authors would like to acknowledge the Utrecht Vascular Cognitive Impairment group. Members of the group involved in this project are M Brundel, LJ Kappelle, YD Reijmer (from the department of Neurology), J de Bresser, HJ Kuijf, WPThM Mali, MA Viergever, and KL Vincken (from the department of Radiology/Image Sciences Institute). Furthermore, the authors thank RLAW Bleys (from the department of Anatomy) for providing the brain slices for protocol optimization.

## REFERENCES

1 Pendlebury ST, Rothwell PM. Prevalence, incidence, and factors associated with pre-stroke and post-stroke dementia: a systematic review and meta-analysis. *Lancet Neurol* 2009; **8**: 1006–1018.
2 Kalaria RN, Kenny RA, Ballard CG, Perry R, Ince P, Polvikoski T. Towards defining the neuropathological substrates of vascular dementia. *J Neurol Sci* 2004; **226**: 75–80.
3 Schneider JA, Arvanitakis Z, Bang W, Bennett DA. Mixed brain pathologies account for most dementia cases in community-dwelling older persons. *Neurology* 2007; **69**: 2197–2204.
4 Pantoni L. Cerebral small vessel disease: from pathogenesis and clinical characteristics to therapeutic challenges. *Lancet Neurol* 2010; **9**: 689–701.
5 Smith EE, Schneider JA, Wardlaw JM, Greenberg SM. Cerebral microinfarcts: the invisible lesions. *Lancet Neurol* 2012; **11**: 272–282.
6 Brundel M, de Bresser J, Van Dillen JJ, Kappelle LJ, Biessels GJ. Cerebral microinfarcts: a systematic review of neuropathological studies. *J Cereb Blood Flow Metab* 2012; **32**: 425–436.
7 White L, Petrovitch H, Hardman J, Nelson J, Davis DG, Ross GW *et al.* Cerebrovascular pathology and dementia in autopsied Honolulu-Asia Aging Study participants. *Ann NY Acad Sci* 2002; **977**: 9–23.
8 Suter OC, Sunthorn T, Kraftsik R, Straubel J, Darekar P, Khalili K *et al.* Cerebral hypoperfusion generates cortical watershed microinfarcts in Alzheimer disease. *Stroke* 2002; **33**: 1986–1992.
9 Tombaugh TN, McIntyre NJ. The mini-mental state examination: a comprehensive review. *J Am Geriatr Soc* 1992; **40**: 922–935.
10 Visser F, Zwanenburg JJM, Hoogduin JM, Luijten PR. High-resolution magnetization-prepared 3D-FLAIR imaging at 7.0 Tesla. *Magn Reson Med* 2010; **64**: 194–202.
11 Busse RF, Hariharan H, Vu A, Brittain JH. Fast spin echo sequences with very long echo trains: design of variable refocusing flip angle schedules and generation of clinical T2 contrast. *Magn Reson Med* 2006; **55**: 1030–1037.
12 Wisse LE, Gerritsen L, Zwanenburg JJ, Kuijf HJ, Luijten PR, Biessels GJ *et al.* Subfields of the hippocampal formation at 7T MRI: *In vivo* volumetric assessment. *Neuroimage* 2012; **61**: 1043–1049.
13 Wahlund LO, Barkhof F, Fazekas F, Bronge L, Augustin M, Sjögren M *et al.* A new rating scale for age-related white matter changes applicable to MRI and CT. *Stroke* 2001; **32**: 1318–1322.
14 Gouw AA, Seewann A, Vrenken H, van der Flier WM, Rozemuller JM, Barkhof F *et al.* Heterogeneity of white matter hyperintensities in Alzheimer's disease: post-mortem quantitative MRI and neuropathology. *Brain* 2008; **131**: 3286–3298.
15 Schmierer K, Parkes HG, So PW, An SF, Brandner S, Ordidge RJ *et al.* High field (9.4 Tesla) magnetic resonance imaging of cortical grey matter lesions in multiple sclerosis. *Brain* 2010; **133**: 858–867.
16 De Reuck J, Auger F, Cordonnier C, Deramecourt V, Durieux N, Pasquier F *et al.* Comparison of 7.0-T $T_2$*-magnetic resonance imaging of cerebral bleeds in post-mortem brain sections of Alzheimer patients with their neuropathological correlates. *Cerebrovasc Dis* 2011; **31**: 511–517.
17 Van Duijn S, Nabuurs RJ, van Rooden S, Maat-Schieman ML, van Duinen SG, van Buchem MA *et al.* MRI artifacts in human brain tissue after prolonged formalin storage. *Magn Reson Med* 2011; **65**: 1750–1758.
18 Jouvent E, Poupon C, Gray F, Paquet C, Mangin JF, Le Bihan D *et al.* Intracortical infarcts in small vessel disease: a combined 7-T postmortem MRI and neuropathological case study in cerebral autosomal-dominant arteriopathy with subcortical infarcts and leukoencephalopathy. *Stroke* 2011; **42**: 27–30.
19 Li Y, Maeda M, Kida H, Matsuo K, Shindo A, Taniguchi A *et al. In vivo* detection of cortical microinfarcts on ultrahigh-field MRI. *J Neuroimaging* 2012, e-pub ahead of print 18 May 2012; doi:10.1111/j.1552-6569.2012.00722.x.

20 Madai VI, von Samson-Himmelstjerna FC, Bauer M, Stengl KL, Mutke MA, Tovar-Martinez E *et al.* Ultrahigh-field MRI in human ischemic stroke - a 7 Tesla study. *PLoS ONE* 2012; **7**: e37631.
21 Kövari E, Gold G, Herrmann FR, Canuto A, Hof PR, Bouras C *et al.* Cortical microinfarcts and demyelination affect cognition in cases at high risk for dementia. *Neurology* 2007; **68**: 927–931.
22 Sonnen JA, Santa Cruz K, Hemmy LS, Woltjer R, Leverenz JB, Montine KS *et al.* Ecology of the aging human brain. *Arch Neurol* 2011; **68**: 1049–1056.
23 Richardson K, Stephan BC, Ince PG, Brayne C, Matthews FE, Esiri MM. The neuropathology of vascular disease in the Medical Research Council Cognitive Function and Ageing Study (MRC CFAS). *Curr Alzheimer Res* 2012; **9**: 687–696.
24 Kalaria RN. Cerebrovascular disease and mechanisms of Cognitive Impairment: evidence from clinicopathological studies in humans. *Stroke* 2012; **43**: 2526–2534.
25 Arvanitakis Z, Leurgans SE, Barnes LL, Bennett DA, Schneider JA. Microinfarct pathology, dementia, and cognitive systems. *Stroke* 2011; **42**: 722–727.
26 Launer LJ, Hughes TM, White LR. Microinfarcts brain atrophy, and cognitive function: the Honolulu Asia Aging Study Autopsy Study. *Ann Neurol* 2011; **70**: 774–780.
27 Deramecourt V, Slade JY, Oakley AE, Perry RH, Ince PG, Maurage CA *et al.* Staging and natural history of cerebrovascular pathology in dementia. *Neurology* 2012; **78**: 1043–1050.
28 Pfefferbaum A, Sullivan EV, Adalsteinsson E, Garrick T, Harper C, Postmortem MR. imaging of formalin-fixed human brain. *Neuroimage* 2004; **21**: 1585–1595.
29 Braak H, Braak E. Neuropathological stageing of Alzheimer-related changes. *Acta Neuropathol* 1991; **82**: 239–259.
30 Braak H, Del Tredici K, Rüb U, de Vos RA, Jansen Steur EN, Braak E. Staging of brain pathology related to sporadic Parkinson's disease. *Neurobiol Aging* 2003; **24**: 197–211.

Supplementary Information accompanies the paper on the Journal of Cerebral Blood Flow & Metabolism website (http://www.nature.com/jcbfm)